

RESEARCH PERFORMANCE PROGRESS REPORT

FEDERAL AGENCY:

U.S. DOE/NETL
NATIONAL ENERGY TECH LAB
3610 Collins Ferry Road
PO Box 880
Morgantown, WV 26507-0880

FEDERAL GRANT OR OTHER IDENTIFYING NUMBER BY AGENCY:

DE-FE0029059

PROJECT TITLE:

Remote Methane Sensor for Emissions from Pipelines and
Compressor Stations Using Chirped-Laser Dispersion Spectroscopy

PI NAME:

Mark Zondlo
Associate Professor of Civil and Environmental Engineering
Email: mzondlo@princeton.edu
Phone: (609) 258-5037
Fax: (609) 258-2760

CO-PI NAME:

Gerard Wysocki
Associate Professor of Electrical Engineering
Email: gwyssocki@princeton.edu

SUBMISSION DATE:

January 31, 2018

DUNS NUMBER: 00-248-4665

RECIPIENT ORGANIZATON:

Princeton University
Princeton, NJ 08544

PROJECT/GRANT PERIOD

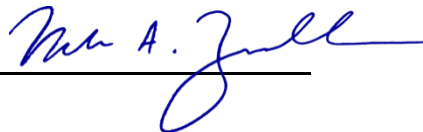
10/1/2016 - 3/31/2018

REPORTING PERIOD END DATE

December 31, 2017

REPORTING TERM OR FREQUENCY

Quarterly (for period 9/1/17 to 12/31/17)



Cover Page (previous)

2. Accomplishments

2a. Goals

Leak rates of methane (CH₄) from the natural gas supply chain result in lost profit from unsold product, public safety and property concerns due to potential explosion hazards, and a potentially large source of economic damages from legal liabilities. Yet large measurement challenges exist in identifying and quantifying CH₄ leak rates along the vast number and type of components in the natural gas supply chain. This is particularly true of the “midstream” components of gathering, processing, compression, transmission, and storage.

This project will develop and deploy new advances in chirped laser dispersion spectroscopy (CLaDS) to make an airborne-based sensor for remote detection of methane leaks from pipelines, compressor stations, and other midstream infrastructure. Leaks of methane not detected through routine pipeline patrols and only inferred by indirect methods (e.g. dead vegetation). The proposed heterodyne-enhanced chirped modulated CLaDS (HE-CM-CLaDS) system will offer ability to perform measurements with low light returns, immunity to back-scattered light intensity fluctuations and high linearity and extended dynamic range of concentration detection.

The proposed effort will use a range-resolved, integrated-path spectroscopic technique to remotely identify leaks along pipelines and other related facilities. The instrument will be capable of being deployed on a vehicle, manned aircraft, or making three-dimensional tomographic images with appropriate flight patterns of a microdrone or by passive sampling. Manned aircraft already patrol pipelines for threat detection and visible signs of leak on monthly timescales. Yet there exist no sensors that can show the necessary sensitivity to detect leaks from such a platform. In this project, we will develop, field test, validate, and demonstrate the system over a pipeline corridor. The system proposed here will target the following specifications:

- Open-path methane measurement
- Sensitivity to methane will be in the $<1\text{ppmv}\cdot\text{m}/\text{Hz}^{1/2}$
- Simultaneous range measurement for 3D tomographic reconstruction
- Ability to perform sensitive CH₄ measurements by scattering from natural hard-targets

The technical innovation is using range-resolved, chirped modulation-chirped laser dispersion spectroscopic detection for methane quantification, which will provide the most robust yet relatively inexpensive hardware solution while delivering sensing performance needed for the target application. The proposed method utilizes optical phase of the detected light for molecular detection and thus is insensitive to fluctuations in intensity of backscattered light within four orders of magnitude, a key feature necessary when scanning through natural hard targets. The proposed system will be validated by controlled tracer releases when integrated onto vehicle and aircraft-based platforms.

Commercial translation to the marketplace will occur by partnering with a pipeline service provider, American Aerospace Technologies, Inc., for flight demonstrations to their clients in the gas, oil, and pipeline industries. In this way, feedback on the sensor performance and attributes

will be efficient and minimize delays in bringing the technologies to the private sector. Benefits of a commercial sensor with these capabilities include reductions of leaks for pipeline operators (more profit), earlier detection of leaks to avoid catastrophic explosion hazards (employee safety, public health and mitigation of property damage), and reduced methane emissions to the atmosphere (improving air quality).

2b. Major activities, results, and outcomes/achievements (Milestone Status Report at end)

Task 1: Project Management, Planning, and Reporting

Status: Completed

Deliverables: Project Management Plan was March 20, 2017 and accepted by the Project Manager via email notification on March 27, 2017.

Milestone A: Data Management Plan submitted → milestone achieved on March 20, 2017.

Task 2: Development of HE-CM-CLaDS sensor

Milestone A: System Developed → on track, planned by February 2018

Research progress made in the last quarter:

- Updated collecting optics design with auto-focusing capability for UAV tracking
- Improved algorithms for range-resolving CLaDS

Task 2.1: Updated collecting optics design for moving target

In the last quarterly report we showed a two-lens system design for auto-focusing, where a concave lens was used to re-collimate the focused image from telescope and a second convex lens was used to refocus the image onto the photodetector. We revisited the optimal requirements for the two-lens system and updated the lens combination accordingly. The two-lens system should be compatible with both reflective target and scattering target with enhancement from an optical local oscillator. The refocused spot size is most desirable to fill the detection element of the photodetector. To maximize heterodyne efficiency for HE-CLaDS, the local oscillator beam shall be reshaped to match the re-collimated beam collected by the telescope. An updated collecting optics design of the two-lens refocusing for the telescope and three-lens beam reshaping for the optical local oscillator (LO) is shown in Figure 1.

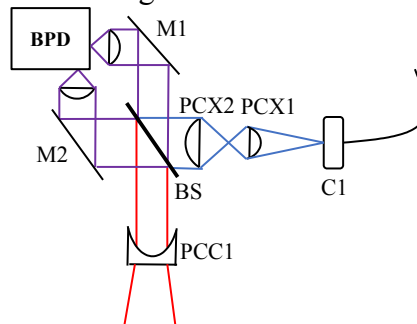


Figure 1. Beam reshaping for HE-CLaDS. BPD-balanced photodetector, M-mirror, BS-beamsplitter, PCX-plano-convex lens, PCC-plano-concave lens, C-collimator.

Task 2.2: CLaDS ranging correction

Three corrections have been implemented to improve the accuracy of the CLaDS ranging functionality since last report:

1. At RF chirping generation side, IQ impairment is added to further suppress unwanted higher order harmonics caused by IQ imbalance in the single sideband mixer.
2. Bidirectional clock signals are created to synchronize RF transceiver, FPGA, and DAQ board for laser modulation together.
3. At RF demodulation side, both phase demodulated and frequency demodulated signals are used to extract ranging information.

The RF chirping generation relies on perfect image cancellation in the single sideband mixer. An alternative way to represent the mixing with imperfection is shown below:

$$T_x(t) = \text{Re}\{A_T(\exp(j\Omega_0 t)\exp(j\Omega_0 t))(G \begin{pmatrix} \cos(2\pi \frac{S_{RF} t^2}{2}) \\ j \sin(2\pi \frac{S_{RF} t^2}{2}) \end{pmatrix} + C)\} \quad (1)$$

Where G is a 2x2 matrix representing gain imbalance and phase skew, and C is a 2x1 vector represents pre-mixer offset, both of which are assumed to occur between DAC and the mixer. If we further assume G and C are fixed, we can counter their effect by introducing baseband correction before DAC. With an assumption of an IQ vector $\begin{pmatrix} \cos(2\pi \frac{S_{RF} t^2}{2}) \\ j \sin(2\pi \frac{S_{RF} t^2}{2}) \end{pmatrix}$ to be X, and the mixer

vector $A_T(\exp(j\Omega_0 t)\exp(j\Omega_0 t))$ to be W^T , Eq. (1) is simplified to $T_x = \text{Re}\{W^T(GX + C)\}$. Since the goal is to obtain $T_x = \text{Re}\{W^T X\}$, the correction can be performed as follows:

$$T_x = \text{Re}\{W^T(G(KX + A) + C)\} = \text{Re}\{W^T(GKX + GA + C)\} \quad (2)$$

with an obvious choice for K and A to be $K = G^{-1}$ and $A = -G^{-1}C$. One way to estimate G and C is to directly tune the parameters for K and A and since G potentially contains complex numbers, to compensate for both amplitude and phase skew doubles the parameters to be tuned empirically. A further simplification is made such that the phase skew $\Delta\xi$ is only caused single-sided (either with I or Q channel), and is corrected through the pre-DAC phase offset. The rest of the algorithm is done through a modified version of IQ impairment function provided by NI Labview. This simplification reduces number of parameters, and shortens the computation clock cycles on the FPGA. Figure 2a shows the updated schematic for IQ impairment.

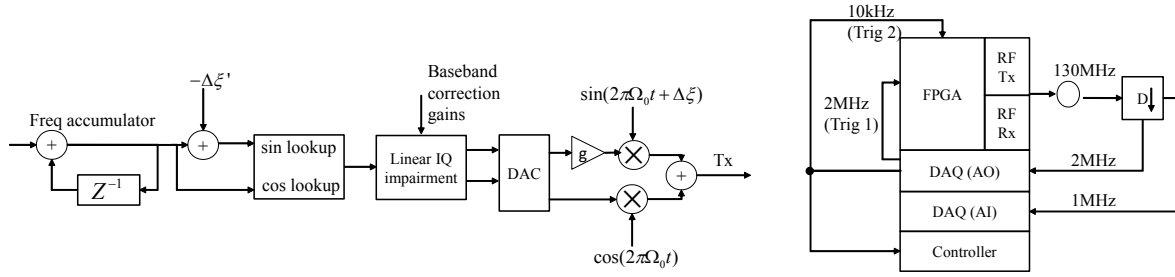


Figure 2. a) IQ impairment with single branch imbalance model and b) cross-device synchronization.

A simplified block diagram in Figure 2b describes the cross-device synchronization. There are four devices integrated on the NI PIXie chassis: DAQ for both modulation generation and analog inputs, PC, FPGA and RF transceiver. The chassis provides a base clock as reference for all devices, but each device is equipped with an independent onboard clock for data sampling, which presumably causes drift overtime. The solution is to create a “feedback” in synchronization. The ADC built-in the RF transceiver has the fastest data clock at 130MS/s which in turn determines the single cycle time loop (SCTL) period in FPGA. A 2MHz clock is created in FPGA by digital downsampling and transferred to the DAQ board as its sampling clock.

As the third improvement, RF phase demodulation is utilized to allow additional correction on the receiver side. The frequency offset in CLaDS corresponds to the linear slope $-S_{RF}\tau t$ in phase demodulated signal, and the phase offset can be extracted after subtracting the linear term. The correction is done by assuming the frequency offset is accurate within half wavelength of the RF carrier:

$$L = \text{round}\left[\frac{(\Delta f - f_0)}{S_{RF}}\Omega_0\right] \frac{c}{\Omega_0} + \frac{(\Delta\phi - \phi_0)}{2\pi\Omega_0} c \quad (3)$$

Due to phase drift the correction needs to be computed in combination with calibration for the phase offset due to initial wiring and optical fiber before free space optics. An RF switch with a second fast photodetector can be used to reassess both frequency and phase initial offsets.

Task 3: Laboratory testing of system parameters

Status: In-progress

Research progress made:

- **Laboratory ranging precision and accuracy test**

Task 3.1: In-lab ranging precision test

A fiber-coupled system with improvements described in Task 2.2 was tested with CM-CLaDS for long-term precision evaluation. Figure 3a shows the time-domain zero-harmonic of frequency demodulated signals with mean offset to zero and the corresponding plot before and after drift elimination. Figure 3b shows the precision evaluated by Allan plots. Shown as the red dotted line in Figure 3b, phase demodulation offers $0.1 \text{ mm/Hz}^{1/2}$ precision compared with $40 \text{ mm/Hz}^{1/2}$ precision using frequency demodulation at the cost of fast drift, therefore a calibration signal is necessary if no active phase stabilization is applied on the circuits.

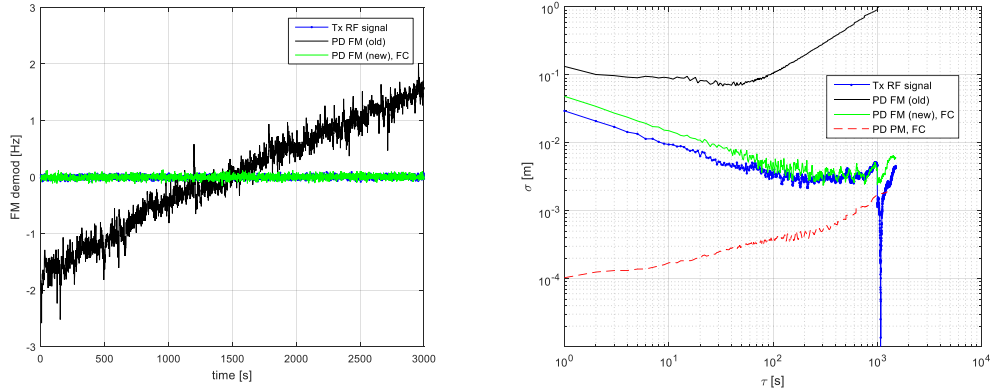


Figure 3. a) Time domain frequency drift before and after synchronization and b) distance precision measured with frequency demodulation and phase demodulation.

An in-lab free space system in Figure 4 was then used to evaluate the accuracy of the ranging capability within 1m path-length difference with a meter stick (± 1 mm) as reference.

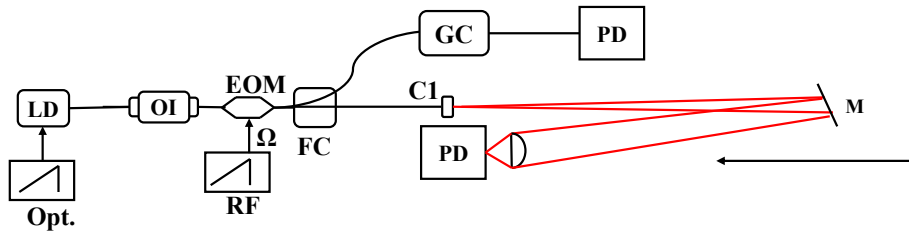


Figure 4. Schematic for in-lab ranging accuracy measurement setup.

Range signals directly converted from frequency offset and phase offset are plotted in Figure 5. The error signal of frequency demodulated range shows a clear periodicity that coincides with the RF carrier frequency, suggesting a pickup or unsuppressed harmonic interference. The phase demodulated accuracy is comparable with the reference, but wraps every 30 cm for 1 GHz RF carrier. Combination of both methods brings down the error to zero if the error by frequency demodulation is within half a wavelength, otherwise the phase correction risks increasing the error as predicted in Task 2.2.

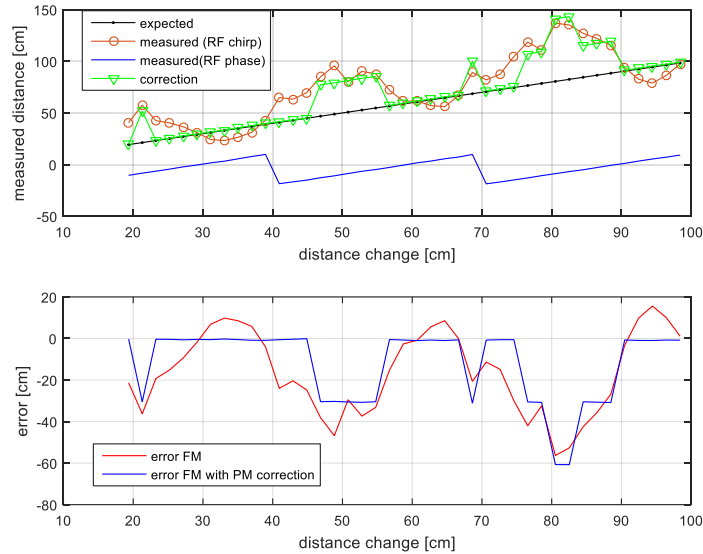


Figure 5. In-lab ranging measurement and error with and without phase correction.

Task 4: outdoor testing and validation of system performance

Status: In progress

Research progress made:

- Stage one testing outside laboratory setting
- Design and development of 100 m roundtrip test facility

Task 4.1: CLaDS remote sensing test and develop 100 outdoor calibration system

The system in Task 2.2 and Task 3 was interfaced with the telescope for remote sensing shown in Figure 6, which is brought to a long hallway for atmospheric methane sensing inside the Engineering building. A LICOR 7700 calibrated point sensor was used in the test to provide reference methane concentration measurement with simultaneous temperature and pressure data. A retroreflector is used as reflective target positioned at a remote location between 8 and 52 m away.

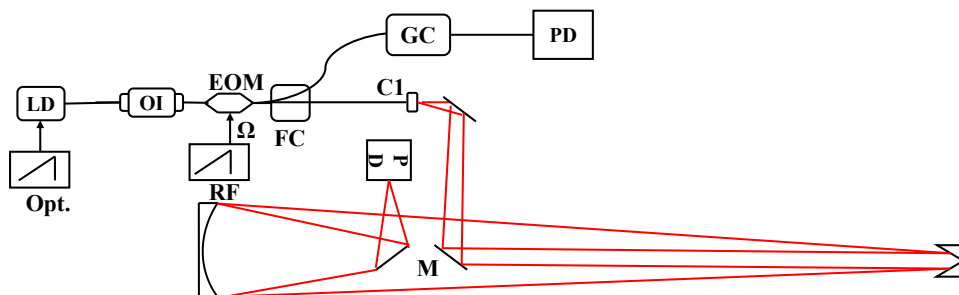


Figure 6. Schematic for range resolving remote sensing CLaDS. LD- laser diode, OI-optical isolator, EOM-electro-optical modulator; RF- RF generator; PD- photodetector; GC-reference gas cell; C1- collimator; M-mirror.

Both direct CLaDS with 10 kHz ramping modulation and CM-CLaDS with 50 kHz modulation have been tested. The optical path with reference gas cell in Figure 6 provides both frequency and phase offset calibration and concentration calibration. With direct CLaDS, the distance

measurement is built into the spectrum fitting model. With CM-CLaDS, 0th harmonic gives frequency demodulated ranging information whereas 2nd harmonic provides absorption through either fitting or on-line calibration.

The range measurement result is plotted against the distance reference in Figure 7a. Phase correction brings down the error in general, which stays below 0.3 m up to 104 m optical path-length with 0.14 m root mean square error, which is on target to achieve the project goal for range-finding resolution set to 0.1m.

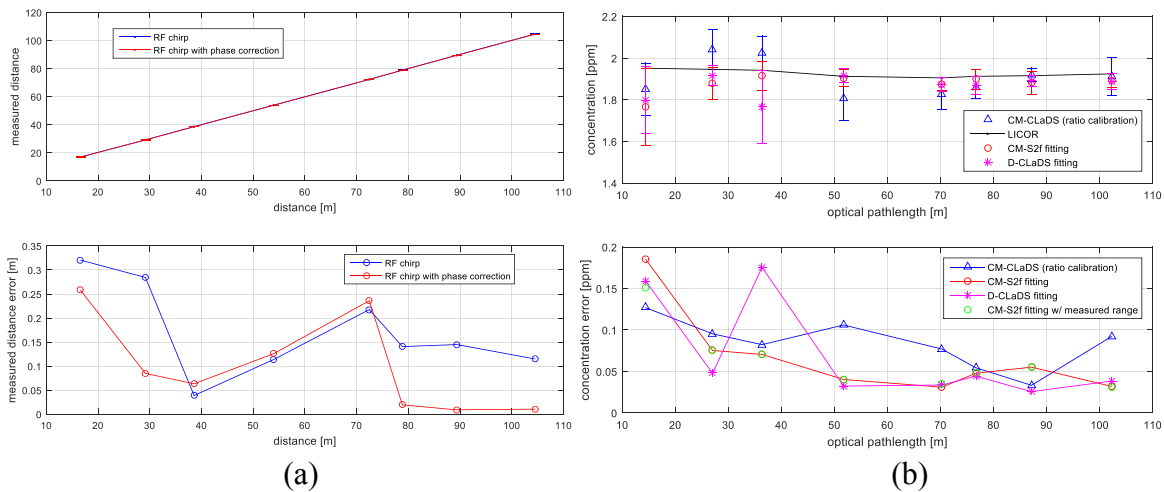


Figure 7. a) Free space ranging measurement up to 100 m optical path-length and the error signals with and without phase correction and b) free space methane concentration measurement and error with single-point CM-CLaDS, second harmonic CM-CLaDS fitting and direct-CLaDS fitting.

The CLaDS concentration retrieval results shown in Fig. 7b is consistent with the LICOR sensor reading for 1.9 ppm methane background with up to 0.2 ppm error for all methods. The concentration can be extracted using either the reference distance measurement with external laser range-finder used in the test or by using the built-in CLaDS ranging measurement. The almost identical green error signal with directly measured distance and red error signal using reference distance by laser ranger shown in Figure 7b imply that ranging accuracy of the CLaDS system has negligible effect on the concentration retrieval. The concentration retrieval accuracy slightly degrades with single-point calibrated CM-CLaDS which was traced to be caused by parasitic fringes in calibration gas cell. The fringe crosstalk is of less impact when using full spectrum fitting with either CM-CLaDS or direct CLaDS.

Development of outdoor testing facility

The CLaDS setup will be tested outside in a controlled environment that mimics signals expected for flight conditions. For conducting these tests outside, a 50 m long and 20 cm diameter bellowed tube will be placed along the wall of a nearby parking garage. A schematic of the system is shown in Fig. 8. The bellowed tubing consists of 6.1 m (20') sections and will be joined together by a custom aluminum coupler with worm clamps. The couplers will have ports for the introduction of calibrated amounts of methane. The sensor and reflector ends of the bellowed tubing will be held by aluminum plates. The sensor end of the tube will be open to the atmosphere where the laser beams will enter and exit the bellowed tubing. The reflector end of the tube will have a place for

a reflector or backscatter target as appropriate and exit ports for the gas flow. Alignment chucks will be placed as necessary to ensure the bellowed tubing is concentric (i.e. not sagging) within 2.54 cm (1") along the 50 m length. The inside of the bellowed tubing is black and will not reflect or scatter infrared light from the laser.

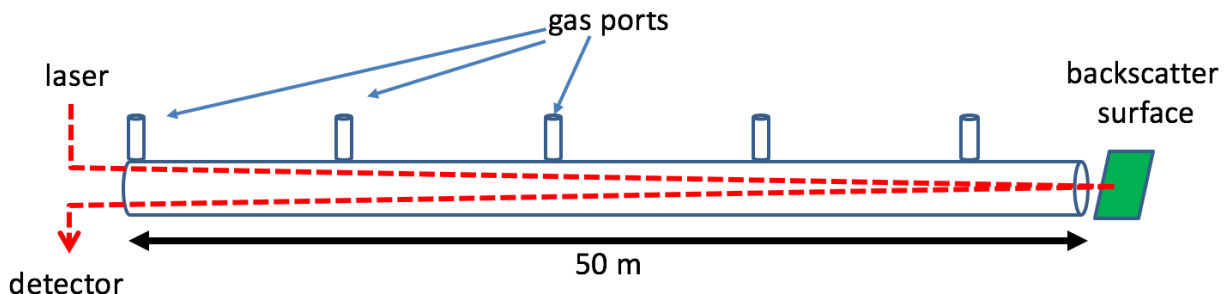


Figure 8. Schematic of the outdoor test facility for conducting CLaDS precision, accuracy, and resolution experiments. A pump will be attached at the downstream (backscatter) end for the dynamic (flowing) experiments. Also not shown is a LICOR LI-7700 methane analyzer on the upstream end to measure ambient methane concentrations on the upstream side.

The first set of experiments to be conducted will consist of static (no flow) conditions at ambient temperatures, pressures, and methane concentrations. The laser beam will reflect off the backscattered surface with various reflectivities returning to the collection optics. With ambient methane at ~ 2.0 ppmv (to be measured by the LICOR) and a 100 m roundtrip pathlength, this yields a path-integrated value of 200 ppmv-m. The backscattered end will use fully reflective optics (e.g. retroreflector) and then decrease the returned signal by four orders of magnitude below that signal (10%, 1%, 0.1% and 0.01% of the fully reflective signal) through adjustments to the retroreflector position. These tests will demonstrate the precision of the signal at various return light intensities. Target sensitivity is 1 ppmv-m or a signal-to-noise ratio of 200:1 at ambient conditions.

The second set of experiments consists of a dynamic (flowing) configuration to simulate leak conditions in the path. Ambient air will be drawn into the front (laser) end of the tube by attaching a large pump on the backside (reflective) plate. Calibrated amounts of ~ 1000 ppmv CH_4 in air will be added at various distances along the tube at the coupling plates. The turbulent flow will mix the calibrated signal downstream of the input port. These experiments will demonstrate the sensitivity of the system to “leak” levels of CH_4 expected along pipelines (i.e. well above ambient, typically in the 500-2000 ppmv-m). It also will demonstrate how the sensor will have uniform sensitivity over a range of distances. Details of the experiments to be conducted were submitted in the Test Plan for Tasks 3 and 4 as an Appendix to the last quarterly project report.

Task 4.2: Calibrate sensor precision, accuracy, and resolution

Status: Not started yet, planned to begin in May 2018

Task 5: Development of tomographic reconstruction algorithms

Status: Not started yet, planned for August 2018

Task 6: Mobile field tests

Status: Not started yet, planned for October 2018

Task 7: Drone-based reflector target imaging

Status: Not started yet, planned for January 2019

Task 8: Airborne flight measurements

Status: Not started yet, planned for July 2019

Milestone Status Report

Milestone Title / Description	Planned completion	Actual completion	Verification method	Comments
A: Data management plan submitted	3/31/17	3/27/17	Accepted by program manager.	
B: System developed	2/28/18			
C: Lab testing completed	8/31/18			
D: Field validation completed	10/31/18			
E: Tomographic algorithms	10/31/19			
F: Mobile field data collected	1/31/19			
G: Drone-based flights	9/30/19			
H: Manned aircraft flights	2/28/20			

Note: all dates extended by 5 month from the original proposal due to delays in paperwork at start but consistent with the relative timeframes in the SOPO with an effective start date of 3/1/17.

2c. Training and development

Not requested.

2d. Dissemination of Results / Outreach

No outreach events have occurred to communities of interest.

2e. Plans for Next Reporting Period

In the next reporting period we will finish the sensor construction and continue laboratory testing of the system. Continued development of the outdoor calibration system will occur with outside tests beginning in May 2018.

3. Products

Publications, conference papers, and presentations

Publications

G. Plant, Y. Chen, and G. Wysocki, "Optical heterodyne-enhanced chirped laser dispersion spectroscopy," *Optics Letters* 42, 2770-2773 (2017).

Books or other non-periodical, one-time publications

None.

Other publications, conference proceedings, and presentations

Y. Chen, G. Plant, and G. Wysocki, "Heterodyne Efficiency in Chirped Laser Dispersion Spectroscopy," in Conference on Lasers and Electro-Optics(Optical Society of America, San Jose, California, 2017), p. SW4L.5.

4. Participants and other collaborators

American Aerospace Technologies Inc., the commercial partner that will be flying the sensor on aircraft in Year 3 and who will fly a drone with a reflecting target in Year 2, has provided advice on aircraft constraints. These constraints play important roles in the overall design of the sensor while there is still time to adjust to any payload issues (or orientation). A conference call is planned in early 2018 to identify any constraints in the design for aircraft flights later in the project.

5. Impact (optional)

Nothing to report at this time.

6. Changes/problems

No changes to the SOPO or technical problems have been encountered. All tasks and milestones remain on schedule and on specification.

7. Special reporting requirements

None.

8. Budgetary information

Follows on next pages.